




Definitive chemoradiotherapy induces T-cell-inflamed tumor microenvironment in unresectable locally advanced esophageal squamous cell carcinoma

Takumi Habu^{1,2,3} · Shogo Kumagai¹ · Hideaki Bando⁴ · Takeshi Fujisawa⁵ · Saori Mishima⁴ · Daisuke Kotani⁴ · Masaki Nakamura⁵ · Hidehiro Hojo⁵ · Shingo Sakashita⁶ · Takahiro Kinoshita² · Tomonori Yano⁷ · Shuichi Mitsunaga^{3,9} · Hiroyoshi Nishikawa^{1,10} · Shohei Koyama^{1,8}  · Takashi Kojima^{4,5}

Received: 19 February 2024 / Accepted: 23 May 2024 / Published online: 31 May 2024
© Japanese Society of Gastroenterology 2024

Abstract

Background Chemoradiotherapy (CRT) modulates the tumor immune microenvironment of multiple cancer types, including esophageal cancer, which potentially induces both immunogenicity and immunosuppression by upregulating the presentation of tumor-specific antigens and immune checkpoint molecules in tumors, respectively. The prognostic effects of immune modification by CRT in esophageal squamous cell carcinoma (ESCC) remain controversial because of the lack of detailed immunological analyses using paired clinical specimens before and after CRT. We

aimed to clarify the immunological changes in the tumor microenvironment caused by CRT and elucidate the predictive importance of clinical response and prognosis and the rationale for the necessity of subsequent programmed cell death protein 1 (PD-1) inhibitor treatment.

Methods In this study, we performed a comprehensive immunological analysis of paired biopsy specimens using multiplex immunohistochemistry before and after CRT in patients with unresectable locally advanced ESCC.

Results CRT significantly increased the intra-tumoral infiltration and PD-1 expression of CD8⁺ T cells and conventional CD4⁺ T cells but decreased those of regulatory T cells and the accumulation of tumor-associated macrophages. Multivariate analysis of tumor-infiltrating T-cell phenotypes revealed that the density of PD-1⁺CD8⁺ T cells in the tumor

Takumi Habu and Shogo Kumagai are contributed equally to this study.

Supplementary Information The online version contains supplementary material available at <https://doi.org/10.1007/s00535-024-02120-z>.

✉ Shohei Koyama
skoyama@east.ncc.go.jp

✉ Takashi Kojima
takojima@east.ncc.go.jp

¹ Division of Cancer Immunology, Research Institute/Exploratory Oncology Research and Clinical Trial Center (EPOC), National Cancer Center, Kashiwa, Chiba, Japan

² Department of Gastric Surgery, National Cancer Center Hospital East, Kashiwa, Chiba, Japan

³ Course of Advanced Clinical Research of Cancer, Juntendo University Graduate School of Medicine, Tokyo, Japan

⁴ Department of Gastroenterology and Gastrointestinal Oncology, National Cancer Center Hospital East, Kashiwa, Chiba, Japan

⁵ Division of Radiation Oncology and Particle Therapy, National Cancer Center Hospital East, Kashiwa, Chiba, Japan

⁶ Division of Pathology, Exploratory Oncology Research and Clinical Trial Center, National Cancer Center, Kashiwa, Chiba, Japan

⁷ Department of Gastroenterology and Endoscopy, National Cancer Center Hospital East, Kashiwa, Chiba, Japan

⁸ Department of Respiratory Medicine and Clinical Immunology, Osaka University Graduate School of Medicine, Suita, Osaka, Japan

⁹ Division of Biomarker Discovery, Exploratory Oncology Research and Clinical Trial Center, National Cancer Center, Kashiwa, Chiba, Japan

¹⁰ Department of Immunology, Nagoya University Graduate School of Medicine, Nagoya, Japan

after CRT could predict a confirmed complete response and favorable survival.

Conclusions This study showed that CRT improved the immunological characteristics of unresectable locally advanced ESCC and identified the density of PD-1⁺CD8⁺ T cells as a predictive factor for prognosis. This finding supports the rationale for the necessity of subsequent PD-1 inhibitor treatment.

Keywords Chemoradiotherapy · Esophageal squamous cell carcinoma · Tumor-infiltrating lymphocytes

Introduction

Esophageal carcinoma is a leading cause of death worldwide [1]. In Western countries, junctional adenocarcinoma accounts for most cases of esophageal carcinoma, whereas squamous cell carcinoma accounts for most cases in Asia, including Japan [2, 3]. Radiation therapy (RT) is a good indication for the treatment of squamous cell carcinoma, and chemoradiotherapy (CRT) is widely accepted as the standard treatment for unresectable locally advanced esophageal squamous cell carcinoma (ESCC), showing efficacy with a complete response (CR) rate of 11–25% and an overall survival (OS) period of 9–10 months. CR on CRT is a strong predictor of survival in ESCC [4–7]. Although new therapeutic strategies other than CRT have been investigated, the standard treatment strategy has not changed over the past 20 years.

Based on the results of KEYNOTE-590 and CheckMate-648, combination therapy, either pembrolizumab plus cytotoxic chemotherapy or nivolumab plus ipilimumab, has become the standard first-line treatment for patients with metastatic esophageal cancer who meet the following criterion: ECOG performance status (PS) of 0–1, with permitted tolerability [8, 9]. In addition, based on the results of CheckMate-577, postoperative nivolumab is now strongly recommended if pathological CR cannot be achieved with neoadjuvant CRT followed by surgery [10]. Recent clinical trials of unresectable locally advanced rectal cancer [11] and stage III non-small cell lung cancer [12] have suggested the importance of adding programmed cell death protein-1 (PD-1) inhibitors after definitive CRT. To develop novel combinatorial strategies for CRT with immune checkpoint inhibitors (ICIs), it is necessary to elucidate how CRT alters the tumor microenvironment (TME) from an immunological perspective.

CRT promotes immune cell infiltration into the TME in esophageal adenocarcinomas [13, 14]. However, few studies have performed comprehensive immunological analyses of tumor samples before and after CRT in patients

with advanced ESCC. In the present study, we performed multiplex immunohistochemistry (mIHC) using paired endoscopic specimens before and after CRT in patients with unresectable locally advanced ESCC. Consequently, we aimed to clarify the immunological changes in the TME caused by CRT and elucidate the predictive importance of clinical response and prognosis and the rationale for the necessity of subsequent PD-1 inhibitor treatment.

Methods

Patients and study criteria

Patients treated with concurrent standard-dose 5-fluorouracil (5-FU)/cisplatin (CDDP) chemotherapy and RT (definitive CRT) at the National Cancer Center Hospital East between January 2013 and March 2020 were enrolled in this study. The eligibility criteria were as follows: (i) patients with histologically confirmed primary ESCC; (ii) patients diagnosed with an unresectable tumor by computed tomography (CT) before initiating definitive CRT (more specifically, [a] the depth of the primary tumor is diagnosed as T4b [tumor invades other adjacent structures, such as the aorta, vertebral body, or trachea] according to the Union for International Cancer Control-tumor-node-metastasis [TNM] classification [8th edition] and Japanese Classification of Esophageal Cancer, 11th Edition, and/or (b) regional lymph nodes and/or supraclavicular lymph nodes have invaded adjacent structures other than the esophagus [LNT4]) [15, 16]; (iii) patients without prior esophageal cancer treatment, except for endoscopic resection before CRT; (iv) patients undergoing post-treatment biopsy 4–6 weeks after RT completion; and (v) patients aged ≥ 20 years. The exclusion criteria were as follows: (i) patients with uncontrolled comorbidities, a history of ischemic heart disease, or active carcinoma at another site and (ii) patients who received induction chemotherapy or participated in clinical trials. ESCC staging was performed using CT and endoscopy. Positron emission tomography–CT was performed when distant metastasis was suspected. Tumor length was measured using a combination of endoscopy and upper gastrointestinal tract radiography. Skilled endoscopists measured the endoscope insertion length from the distal to the proximal side of the tumor.

Definitive chemoradiotherapy and sample collection

The regimen of definitive CRT was two courses of 5-FU/CDDP (70 mg/m² CDDP on day 1 plus 700 mg/m² 5-FU on days 1–4 every 28 days). Consolidation chemotherapy was administered after the completion of definitive CRT if patients did not have local progression or distant metastases

and had adequate organ function. This treatment consisted of two additional courses of 5-FU/CDDP. A total dose of 60 Gy/30 fractions of RT was delivered over 5–7 weeks, and the end date of CRT was defined as the end date of RT. The gross tumor volume was defined as the volume of the primary tumor, as indicated on CT and/or endoscopy, and of any metastatic lymph nodes. The clinical target volume (CTV) for the primary tumor was created by adding a 2-cm craniocaudal margin to account for subclinical tumor extension. The CTV margin for metastatic lymph nodes was not included in the selective irradiation of regional lymph nodes. The planning target volume was defined as the CTV plus the margins at the discretion of the treating radiation oncologists. No prophylactic irradiation was administered. Samples were collected by endoscopic biopsies 2–4 weeks before CRT and 6–8 weeks after CRT. Endoscopic biopsy specimens were taken from the center of all tumors.

Evaluation of therapeutic response and follow-up

CT and endoscopy were used to determine a therapeutic response based on the Response Evaluation Criteria in Solid Tumors (RECIST) version 1.1 with modifications and the Japanese Classification of Esophageal Cancer (11th edition), respectively [16, 17]. The modified RECIST defines both measurable and nonmeasurable lymph nodes as those ≥ 10 mm and 5–10 mm in their short axis, respectively, when assessed by CT [15]. According to the Japanese Classification of Esophageal Cancer, we defined the primary lesion as CR when the conditions satisfied all the following four factors: (1) disappearance of endoscopic findings suggestive of tumor presence, (2) negative endoscopic biopsy findings from the original area of the primary tumor, (3) evaluation of the entire esophagus using endoscopy, and (4) no endoscopic findings of active esophagitis. Confirmed CR (cCR) was defined as the confirmation of CR > 4 weeks after the first CR diagnosis. Progression-free survival (PFS) was defined as the period from the initiation of definitive CRT to progression or death from any cause and was censored on the last day the patient was alive without progression or distant metastases. OS was defined as the period from the initiation of definitive CRT to death from any cause and was censored on the last day the patient was alive. Metachronous esophageal cancers were not included in the PFS analysis.

Multiplex immunohistochemistry

Fluorescent mIHC was performed using the Opal 6-color tyramide signaling amplification kit (Akoya Biosciences, Marlborough, MA). Cells were stained with antibodies against CD3 (ab16669, Abcam, Cambridge, UK), CD8 (M710301-2, Agilent, Santa Clara, CA), FoxP3 (ab96048, Abcam,

Table 1 Clinicopathological patient characteristics

Variables	Total (N = 36)
Age (median), years	66 (42–80)
Sex (male/female)	28/8 (78%/22%)
Smoke (ever/never)	6/30 (17%/83%)
ECOG performance status (0/1)	23/13 (64%/36%)
Primary tumor site (Ce/Ut/Mt/Lt)	6/12/13/5 (17%/33%/36%/14%)
Tumor status (T1/T3/T4b)	1/12/23 (3%/33%/64%)
Adjacent organ invasion via lymph node	16 (44%)
Lymph node status (N0/N1/N2/N3)	1/8/17/10 (3%/22%/47%/28%)
Metastatic stage (M0/M1)	21/15 (58%/42%)
Clinical stage (III/IVA/IVB)	7/14/15 (19%/39%/42%)
Tumor length (median), cm	6.5 (3–14)
Lymph node short diameter (median), mm	14.5 (6–39)
Obstruction (tube feeding)	7 (19%)
Involved sites of T4*	
Aorta	16 (44%)
Tracheobronchial tree	22 (61%)
Others	2 (6%)
Fistula formation (before CRT)	3 (8%)
Ccr (median), mL/min	77 (39–125)

ECOG Eastern Cooperative Oncology Group, Ccr creatinine clearance

*The following factors are allowed to be duplicated

Cambridge, UK), cytokeratin (ARG56129, Arigo Biolaboratories, Hsinchu, Taiwan), PD-1 (ab137132, Abcam, Cambridge, UK), TIGIT (ab243903, Abcam), LAG3 (NBPI-97657, Novus, Cambridge, UK), TIM3 (45208S, Cell Signaling Technology, Danvers, CA), CTLA-4 (ab251599, Abcam, Cambridge, UK), and CD206 (MA5-34981, Thermo Fisher Scientific, Waltham, MA). Moreover, the fluorescence signals were captured with the following fluorophores: Opal 520, Opal 540, Opal 570, Opal 620, Opal 650, and Opal 690, following the manufacturer's protocol (Online Resource 1). Briefly, we prepared tissues for detection with Opal using standard fixation and embedding techniques. Each slide was baked in the oven at 65 °C for 1 h, dewaxed with xylene (3 × 10 min), and rehydrated through a graded series of ethanol solutions (100%, 1 × 10 min; 95%, 1 × 10 min; and rinsed in 70%). After rehydration, we briefly rinsed the slides with distilled water and subsequently with the appropriate AR buffer. We placed each slide in a microwave oven and, subsequently, cooled them back to room temperature. The tissue sections were covered with a blocking buffer, and the slides were incubated in a humidified chamber for 10 min at room temperature. We drained off the blocking buffer and applied a primary antibody working solution. We incubated the tissue sections with primary antibodies according to the manufacturer's instructions and washed the slides thrice in

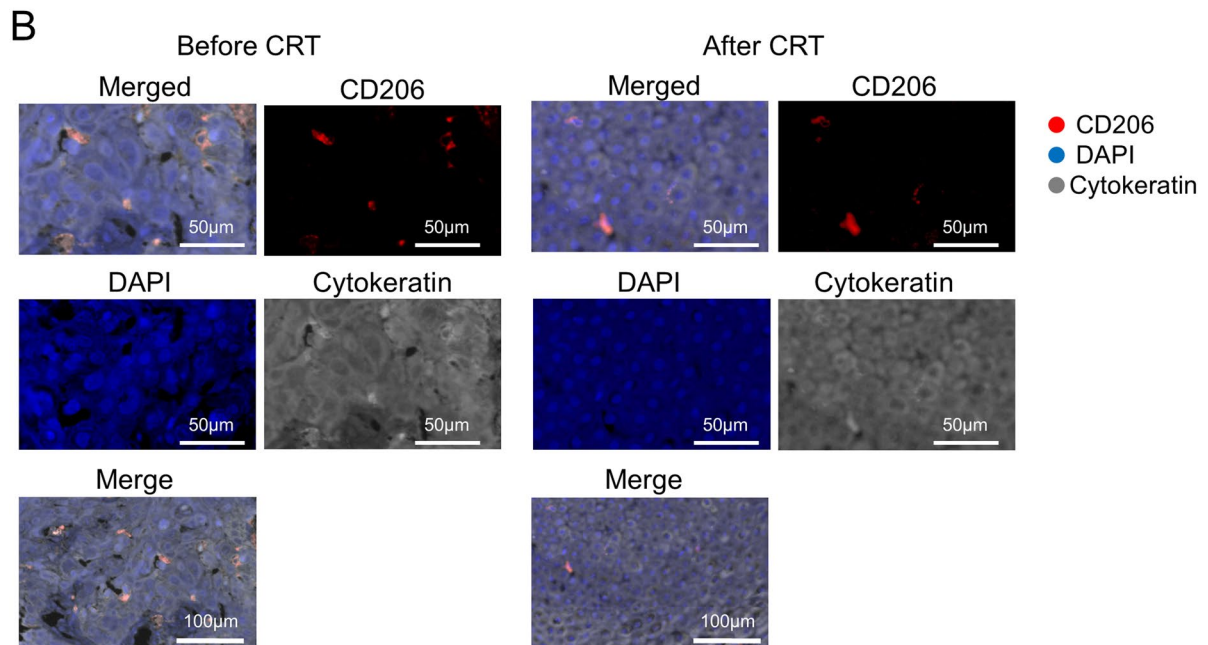
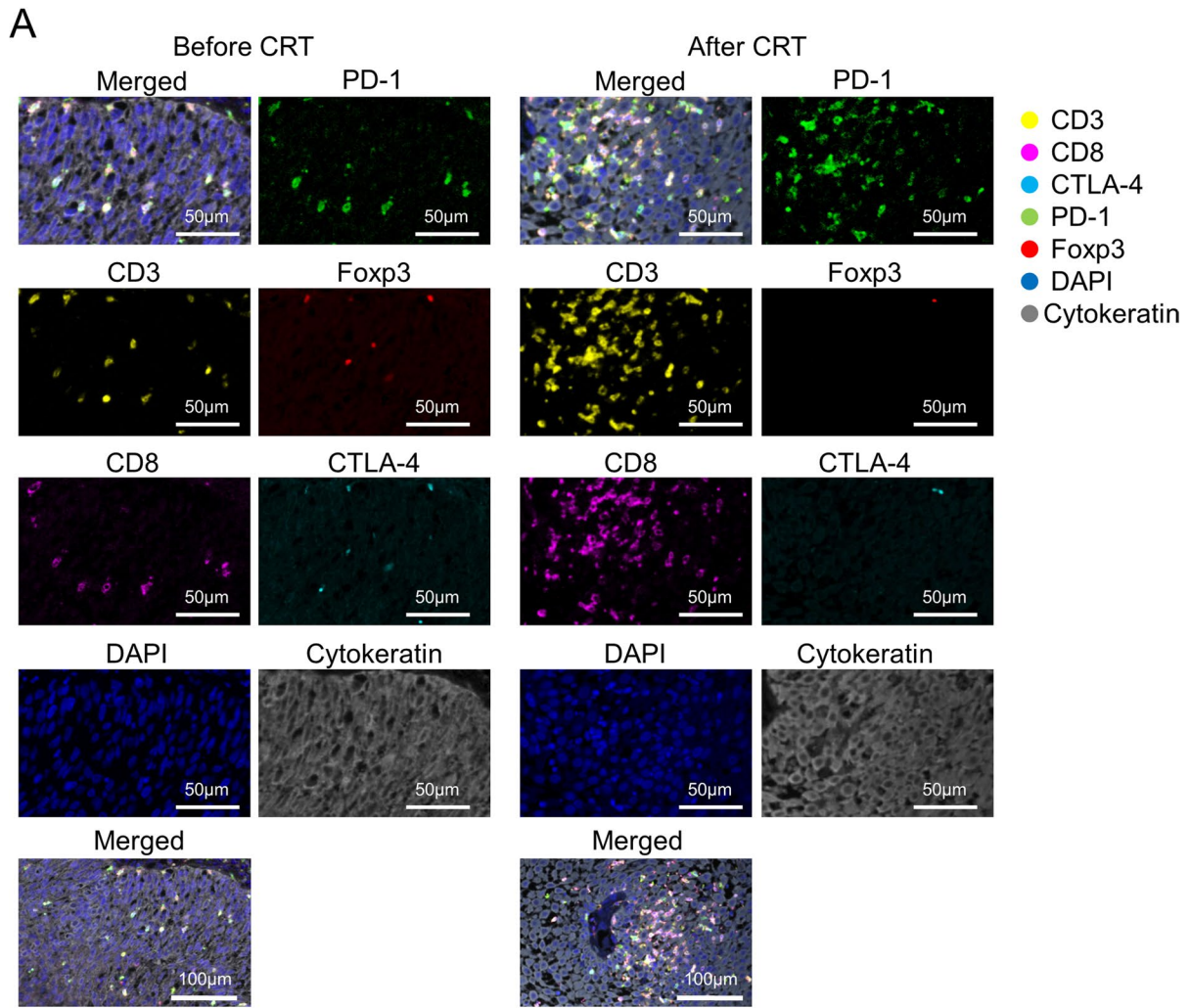


Fig. 1 Representative images of mIHC for ESCC tissues. Representative mIHC images are shown. ESCC tissue samples before and after chemoradiotherapy (left and right) were subjected to mIHC. **A** T-cell-related molecules were evaluated. The stainabilities of CD3 (yellow), CD8 (pink), CTLA-4 (cyan), PD-1 (green), FoxP3 (red), DAPI (blue), and cytokeratin (gray) are shown. **B** Macrophage-related molecules were evaluated. The stainabilities of CD206 (red), DAPI (blue), and cytokeratin (gray) are shown

Tris Buffered Saline Buffer with Tween 20 (TBST) at room temperature, preferably with agitation. We incubated the slides in Polymer HRP Ms + Rb for 10 min at room temperature and washed them thrice in TBST at room temperature, preferably with agitation. We drained off excess wash buffer and pipette 100–300 μ L of Opal Fluorophore Working Solution onto each slide. We incubated the slides at room temperature for 10 min and washed them thrice in TBST at room temperature, preferably with agitation. The slides were rinsed with the appropriate AR buffer. We placed the slides in the appropriate AR buffer, placed them in a microwave, and cooled them to room temperature to strip the primary–secondary–HRP complex, allowing the introduction of the next primary antibody. To detect the next target, we restarted the protocol during the blocking step. After all the targets were processed, we applied the DAPI Working Solution for 5 min at room temperature in a humidity chamber and washed the slides for 2 min in TBST buffer and then for 2 min in water. Finally, we cover-slipped slides with a mounting medium [ProLong[®] Diamond Antifade Mountant (ThermoFisher)]. Visualization of seven-color Opal slides was visualized using the Vectra 3 Automated Quantitative Pathology Imaging System (Akoya Biosciences, Marlboro, MA, USA).

Slide scanning and image analysis

Fluorescence images were acquired using the inForm 2.4.4 image analysis (IA) software (Perkin Elmer). Whole-slide images were analyzed using the IA software (HALO version 2.3; Indica Labs, Corrales, NM) and divided into individual cells based on the expression of stained markers. The slides were manually annotated to remove tissue artifacts (e.g., folds, air bubbles, fluorescent precipitate) and select regions of interest for IA when applicable. A visually adjusted intensity threshold was set for each marker. Cells showing staining intensities above this threshold were considered “positive.” Spots were automatically identified and segmented using the IA software and reviewed by the researchers. The density of stained cells per mm^2 was calculated by dividing the measured area of each tissue spot.

Statistical analyses

The median tumor length, lymphocyte count, and density of tumor-infiltrating lymphocytes (TILs) were used to divide the patients into two groups. TIL levels between pre- and post-treatment biopsy specimens were compared using paired *t* tests. Univariate logistic regression analyses were performed to determine the association between independent variables, and multivariate logistic regression analyses using a backward stepwise selection method were performed to predict cCR. Survival was calculated using the Kaplan–Meier method and compared using the log-rank test. Cox proportional hazards regression analysis for PFS was used for analyses. All statistical analyses were performed using the PRISM software (GraphPad Software Inc., San Diego, CA, USA) and EZR (Saitama Medical Center, Jichi Medical University, Saitama, Japan), a graphical user interface for R 2.13.0 (R Foundation for Statistical Computing, Vienna, Austria) [18]. EZR is a modified version of the R commander (version 1.6–3) designed to add statistical functions that are frequently used in biostatistics. A *P* value of 0.05 was considered statistically significant.

Results

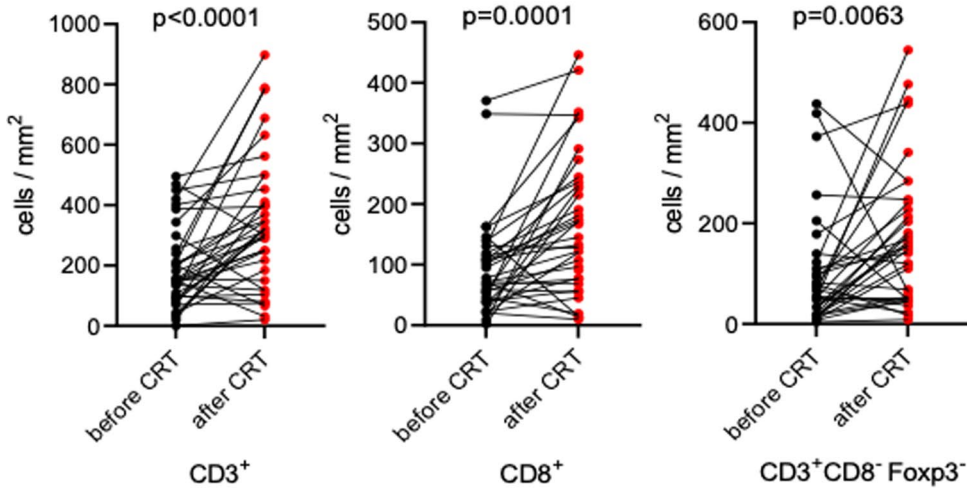
Patient characteristics

Thirty-six patients who received definitive CRT for unresectable locally advanced ESCC were enrolled in this study. Patient characteristics are shown in Table 1. The patients' median age was 66 (range 42–80) years, and 64% of the participants had a PS score of 0. Twenty-three patients had T4b disease, and 16 patients had LNT4 disease. The lesions with tumor invasion were located in the thoracic aorta (44%), trachea/bronchus (61%), and others (5%). Three patients had an invasion of both the thoracic aorta and trachea/bronchus. The median length of the primary lesion was 6.5 (range 3–14) cm. All patients completed two cycles of chemotherapy, and 34 (94%) patients received at least one cycle of consolidation chemotherapy following definitive CRT. cCR was achieved in nine of the 36 (25%) patients. The median PFS and OS periods of the 36 patients were 8 and 18 months, respectively, and the median follow-up periods were 39.5 and 31 months, respectively.

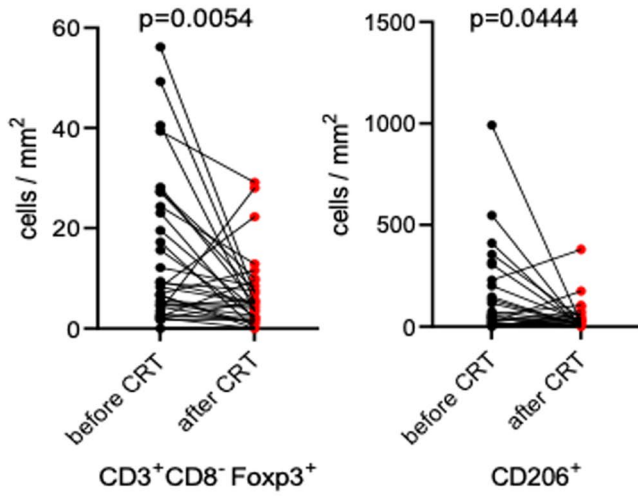
The effects of CRT on the immunological phenotype of TILs

After CRT, the densities of CD3⁺ cells (total T cells), CD3⁺CD8⁺ cells (CD8⁺T cells), and CD3⁺CD8⁺FoxP3⁺ cells (conventional CD4⁺T [Tconv] cells) in the cytokeratin⁺

A



B



C

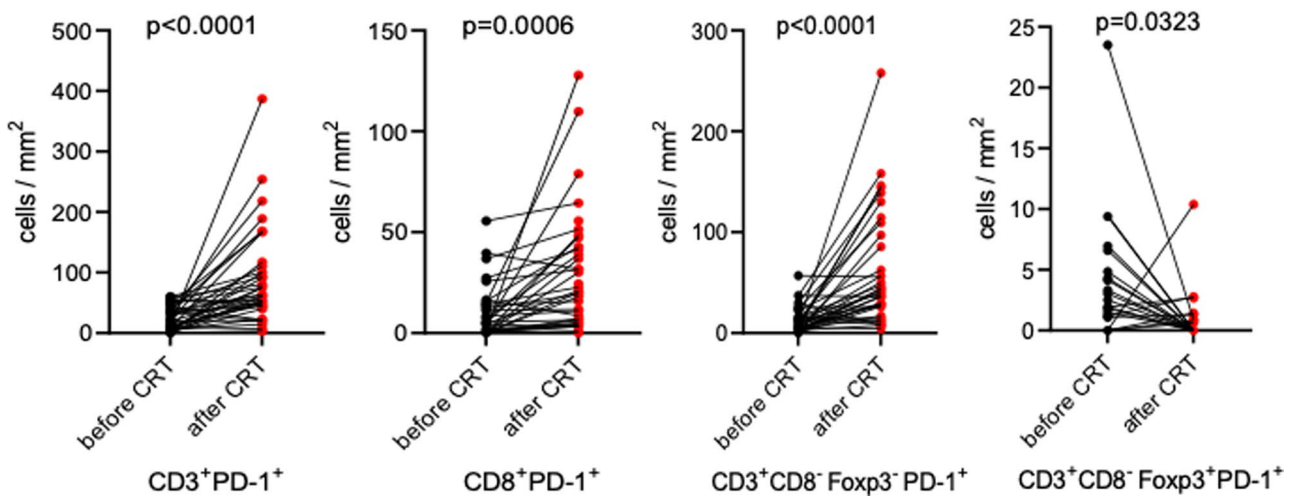


Fig. 2 Effects of CRT on TIL phenotypes. We evaluated the changes in TIL phenotypes caused by CRT. The densities of each TIL subpopulation before and after CRT were compared using a paired *t* test. **A** The densities of CD3⁺ (left), CD3⁺CD8⁺ (middle), and CD3⁺CD8⁻FoxP3⁻ (right) lymphocytes before and after CRT are shown. **B** The densities of CD3⁺CD8⁻FoxP3⁺ lymphocytes (left) and CD206⁺ macrophages (right) before and after CRT are shown. **C** The densities of CD3⁺PD-1⁺, CD3⁺CD8⁺PD-1⁺, and CD3⁺CD8⁻FoxP3⁻PD-1⁺ cells and CD3⁺CD8⁻FoxP3⁺PD-1⁺ lymphocytes before and after CRT

tumor area were significantly elevated (Figs. 1A and 2A), whereas the densities of CD3⁺CD8⁻FoxP3⁺ cells (regulatory T [Treg] cells) and CD206⁺ cells (immunosuppressive macrophages) in the tumor area significantly decreased (Figs. 1A and 2B). Focusing on PD-1 expression in each cell subset, the densities of CD3⁺PD-1⁺ cells (PD-1⁺ total T cells), CD3⁺CD8⁺PD-1⁺ cells (PD-1⁺CD8⁺ T cells), and CD3⁺CD8⁻FoxP3⁻PD-1⁺ cells (PD-1⁺ Tconv cells) significantly increased, whereas the density of CD3⁺CD8⁻FoxP3⁺PD-1⁺ cells (PD-1⁺Treg cells) significantly decreased in the tumor area after CRT (Fig. 2C). Consistent with these results, CRT increased the positivity of PD-1 in tumor-infiltrating CD3⁺, CD3⁺CD8⁺, and CD3⁺CD8⁻FoxP3⁻ cells and reduced the positivity of PD-1 in tumor-infiltrating CD3⁺CD8⁻FoxP3⁺ cells (Online Resource 2A). The expression of other immune checkpoint molecules, including TIGIT, LAG-3, and Tim-3, among CD3⁺CD8⁺PD-1⁺ cells, was not altered (Online Resource 2B); however, the density of CD3⁺CD8⁻FoxP3⁺CTLA-4⁺ cells (CTLA-4⁺ Treg cells) was significantly reduced after CRT in the tumor bed (Online Resource 2C).

CRT increased PD-1⁺CD8⁺ T cells and PD-1⁺ Tconv cells in the TME of patients with cCR

We evaluated the phenotypes of TILs before CRT according to the clinical outcomes (cCR vs. non-cCR) (Online Resource 3). There were no significant differences in the densities of CD3⁺, CD3⁺CD8⁺, CD3⁺CD8⁻FoxP3⁻, and CD3⁺CD8⁻FoxP3⁺ cells and CD206⁺ macrophages in the tumor area between patients with cCR and non-cCR before CRT (Online Resource 3A, B). Similarly, there was no significant difference in the density of PD-1⁺ cells in any subpopulation of the tumor area between patients with cCR and non-cCR before CRT (Online Resource 3C).

The phenotypes of TILs after CRT were also evaluated according to the clinical outcomes (Fig. 3). There were no significant differences in the densities of CD3⁺, CD3⁺CD8⁺, CD3⁺CD8⁻FoxP3⁻, and CD3⁺CD8⁻FoxP3⁺ cells, CD206⁺ macrophages, and CD3⁺CD8⁻FoxP3⁺PD-1⁺ cells between the two groups (Fig. 3A–C). However, the densities of CD3⁺PD-1⁺, CD3⁺CD8⁺PD-1⁺, and

CD3⁺CD8⁻FoxP3⁻PD-1⁺ cells after CRT were significantly elevated in patients with cCR (Fig. 3C).

Abundance of PD-1⁺CD8⁺ T cells after CRT was an independent predictor of cCR

The prognostic effect of each clinicopathological factor on cCR was evaluated using logistic regression analysis (Table 2). As the densities of CD3⁺CD8⁻PD-1⁺, CD3⁺CD8⁺PD-1⁺, CD3⁺CD8⁻FoxP3⁺ cells, and CD206⁺ macrophages after CRT were significantly associated with cCR in univariate analysis (Table 2), we further evaluated them by multivariate analyses. Multivariate analysis of these TIL phenotypes revealed that the density of CD3⁺CD8⁺PD-1⁺ cells in the tumor area after CRT was an independent predictor of cCR (odds ratio [OR], 28.30; 95% confidence interval [CI], 1.32–605.00; *P* = 0.032) (Table 2).

Low density of CD3⁺CD8⁻FoxP3⁺ was associated with favorable PFS both before and after CRT

The association between TIL phenotypes before CRT and patient survival was evaluated using the Kaplan–Meier analysis. Most TIL phenotypes before CRT were not significantly associated with PFS (Online Resource 4A–F, H), but the low densities of CD3⁺CD8⁻FoxP3⁺ showed a statistically favorable prognosis (Online Resource 4G). We further evaluated the prognostic effect of TIL phenotypes on PFS after CRT (Fig. 4). Patients with a high density of CD3⁺CD8⁺PD-1⁺ cells had a favorable prognosis (Fig. 4C), whereas those with a high density of CD3⁺CD8⁻FoxP3⁺ cells or CD206⁺ macrophages had an unfavorable prognosis (Fig. 4G, H). The densities of CD3⁺, CD3⁺PD-1⁺, CD3⁺CD8⁺, CD3⁺CD8⁻FoxP3⁻, and CD3⁺CD8⁻FoxP3⁻PD-1⁺ cells in the tumor area after CRT were not significantly associated with prognosis.

Univariate and multivariate analyses revealed factors associated with favorable PFS

The densities of CD3⁺CD8⁻FoxP3⁺ cells in the tumor area before CRT were significantly associated with unfavorable PFS in univariate analysis. In addition, the densities of CD3⁺CD8⁺PD-1⁺ and CD3⁺CD8⁻FoxP3⁺ cells and CD206⁺ macrophages after CRT were significantly associated with PFS in the univariate analysis (Table 3). Thus, these factors were selected for multivariate analyses, and the density of CD3⁺CD8⁺PD-1⁺ in the tumor area after CRT was an independent predictor of favorable PFS (hazard ratio [19], 0.33; 95% CI 0.14–0.77; *P* = 0.010) (Table 3).

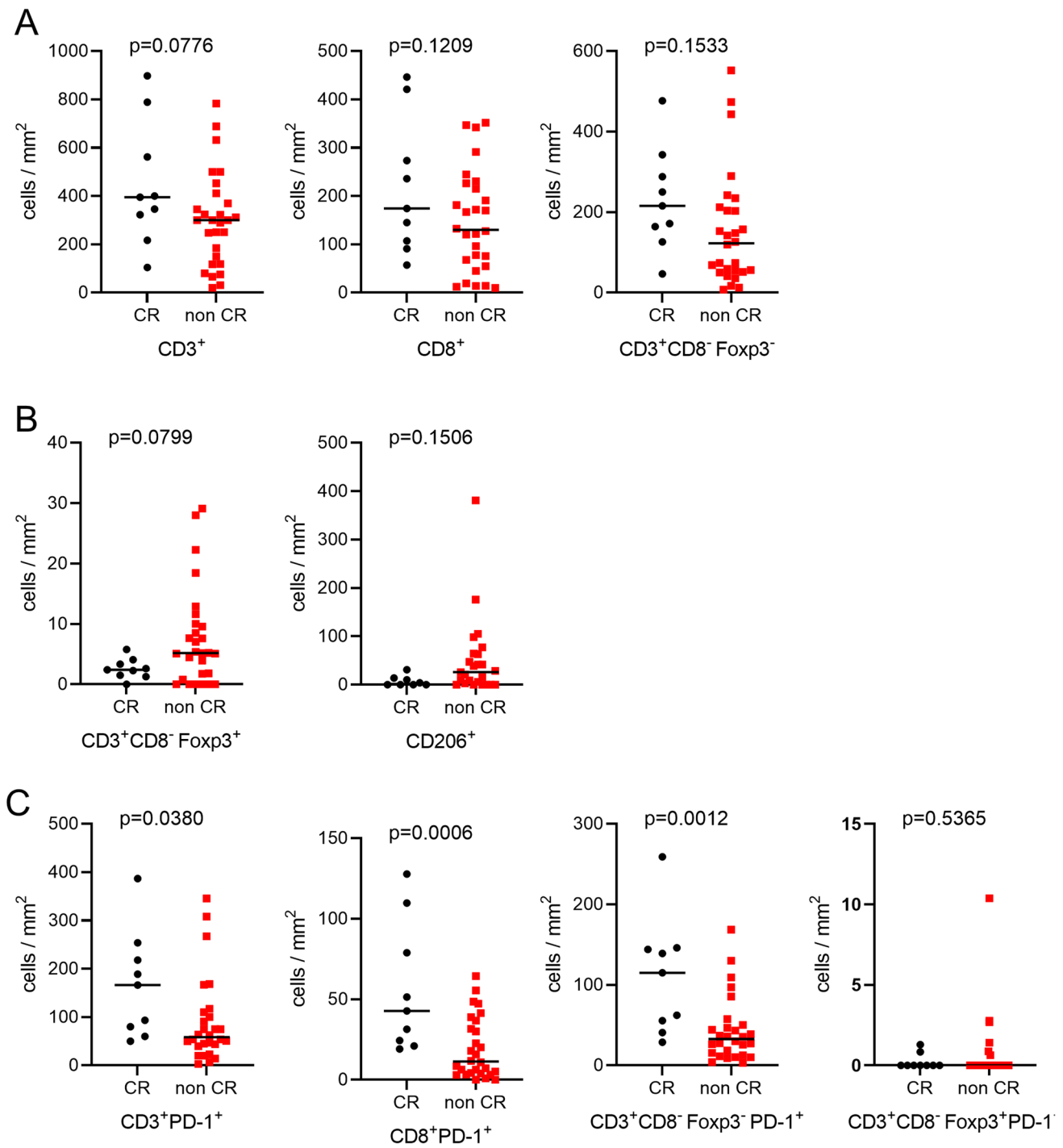


Fig. 3 Association between TIL phenotypes after CRT and confirmed complete response. The densities of the TIL subpopulations after CRT were compared between patients who experienced cCR and those who did not. **A** The densities of CD3⁺ (left), CD3⁺CD8⁺ (middle), and CD3⁺CD8⁻Foxp3⁻ (right) lymphocytes after CRT were compared between the two groups. **B** The densities

of CD3⁺CD8⁻Foxp3⁺ lymphocytes (left) and CD206⁺ macrophages (right) after CRT were compared between the two groups. **C** The densities of CD3⁺PD-1⁺, CD3⁺CD8⁺PD-1⁺, CD3⁺CD8⁻Foxp3⁻PD-1⁺, and CD3⁺CD8⁻Foxp3⁺PD-1⁺ lymphocytes after CRT were compared between the two groups

Discussion

Several studies have investigated the effects of CRT on the

immunological phenotypes of tumors, including ESCC [20]. In preclinical models, CRT causes immunogenic cell death, which induces cancer cells to release tumor-specific

Table 2 Significance of clinicopathologic parameters and immune markers for cCR in patients with unresectable locally advanced ESCC

Variables		Univariate analysis		
		OR	95% CI	P value
Age	≥ 65	1.18	0.24–5.77	0.841
Sex	Male	0.46	0.08–2.47	0.361
Tumor length, cm	≥ 6.5	0.40	0.08–1.94	0.258
Lymphocyte count (before CRT) *	≥ 1470	1.25	0.28–5.65	0.772
Lymphocyte count (after CRT) *	≥ 380	4.04	0.71–23.0	0.115
TIL phenotype before CRT				
CD3 ⁺ , /mm ²	≥ 150	1.73	0.36–8.35	0.493
CD3 ⁺ PD-1 ⁺ , /mm ²	≥ 20	4.04	0.71–23.00	0.115
CD3 ⁺ CD8 ⁻ , /mm ²	≥ 69	1.25	0.28–5.65	0.772
CD3 ⁺ CD8 ⁻ PD-1 ⁺ , /mm ²	≥ 9	0.89	0.42–1.88	0.768
CD3 ⁺ CD8 ⁺ , /mm ²	≥ 70	1.25	0.28–5.65	0.772
CD3 ⁺ CD8 ⁺ PD-1 ⁺ , /mm ²	≥ 4	4.67	0.82–26.60	0.082
CD3 ⁺ CD8 ⁻ Foxp3 ⁺ , /mm ²	≥ 3	0.25	0.04–1.41	0.115
CD206 ⁺ , /mm ²	≥ 30	0.99	0.99–1.00	0.655
TIL phenotype after CRT				
CD3 ⁺ , /mm ²	≥ 312	4.67	0.82–26.60	0.083
CD3 ⁺ PD-1 ⁺ , /mm ²	≥ 63	5.41	0.95–31.00	0.057
CD3 ⁺ CD8 ⁻ , /mm ²	≥ 148	4.67	0.82–26.60	0.083
CD3 ⁺ CD8 ⁻ PD-1 ⁺ , /mm ²	≥ 39	14.40	1.57–132.0	0.018
CD3 ⁺ CD8 ⁺ , /mm ²	≥ 145	2.31	0.48–11.10	0.297
CD3 ⁺ CD8 ⁺ PD-1 ⁺ , /mm ²	≥ 20	12.40	1.35–113.00	0.026
CD3 ⁺ CD8 ⁻ Foxp3 ⁺ , /mm ²	≥ 5	0.06	0.007–0.58	0.015
CD206 ⁺ , /mm ²	≥ 14	0.11	0.01–0.99	0.049
Variables		Multivariate analysis		
		OR	95% CI	P value
TIL phenotype after CRT				
CD3 ⁺ CD8 ⁻ PD-1 ⁺ , /mm ²	≥ 39	16.60	0.79–349.00	0.0708
CD3 ⁺ CD8 ⁺ PD-1 ⁺ , /mm ²	≥ 20	28.30	1.32–605.00	0.0324
CD3 ⁺ CD8 ⁻ Foxp3 ⁺ , /mm ²	≥ 5	0.16	0.008–2.99	0.2190
CD206 ⁺ , /mm ²	≥ 14	0.06	0.002–1.43	0.0824

P value < 0.05 was considered statistically significant

antigens and triggers an antitumor immune response through multiple mechanisms. RT alone stimulates the cyclic guanosine monophosphate–adenosine monophosphate synthase stimulator of interferon (IFN) gene-dependent nucleic acid-sensing pathway, which promotes antigen presentation in cancer cells and dendritic cells (DCs) [21] and cytotoxic T-cell recruitment through IFN-inducible chemokines [19]. Chemotherapies also induce the release of damage-associated molecular patterns, including high-mobility group box-1 protein [22], which activates DCs by binding to Toll-like receptor 4 [23]. These findings suggest that CRT inhibits tumor growth by physically killing tumor cells and optimizing the antitumor immune system. However, DNA damage induced by RT upregulates programmed cell death ligand 1 (PD-L1) expression in cancer cells through the

STAT1/3-IRF1 signaling pathway [24], which potentially contributes to immune evasion by tumor cells. Therefore, the necessity of targeting the PD-1:PD-L1 interaction has been proposed to maintain therapeutic efficacy.

To validate these preclinical results in patient samples, several clinical studies have analyzed esophageal cancer samples, mainly in the neoadjuvant setting. First, several studies focusing on patients with esophageal adenocarcinoma who received neoadjuvant CRT and underwent surgical resection demonstrated that neoadjuvant CRT promoted T-cell infiltration [13, 14]. However, the association between CD8⁺ cell infiltration and clinical outcomes after neoadjuvant CRT remains controversial, with both favorable [25, 26] and poor outcomes [27]. Second, there are a few studies on patients with ESCC who received neoadjuvant

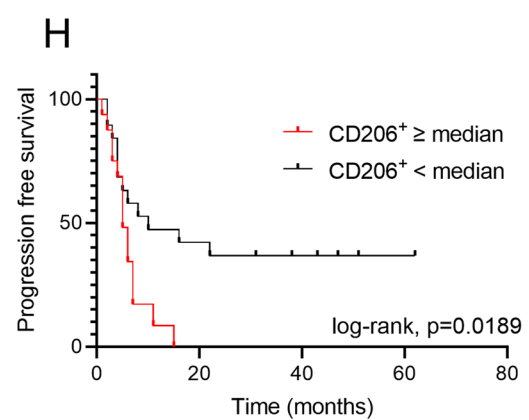
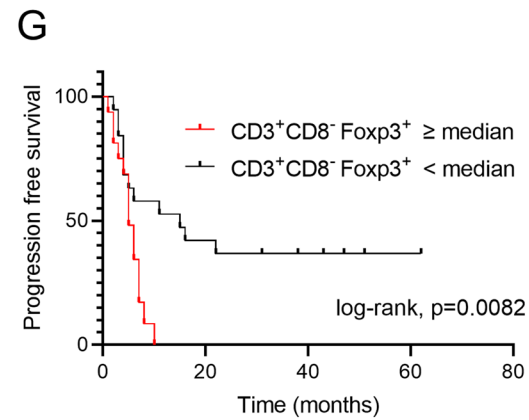
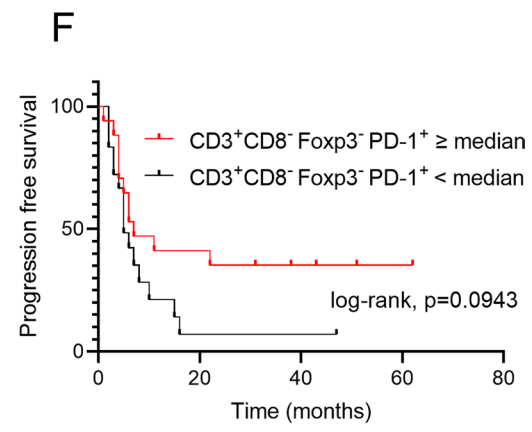
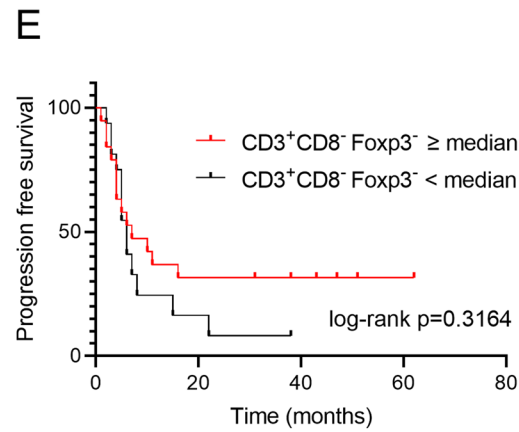
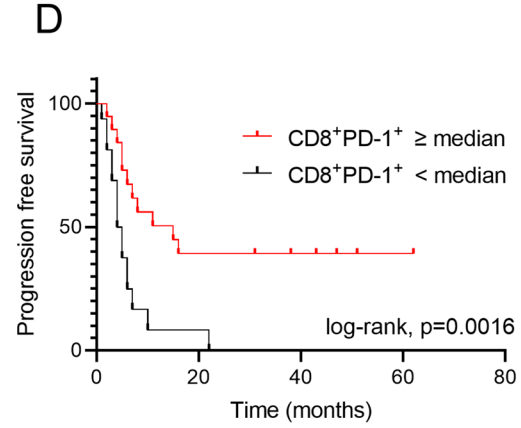
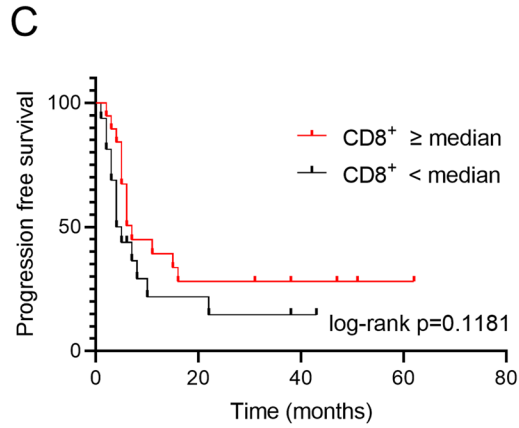
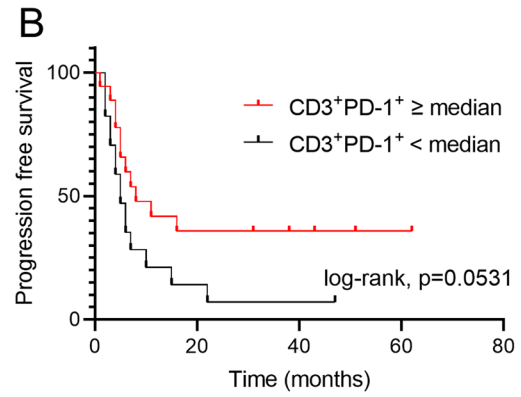
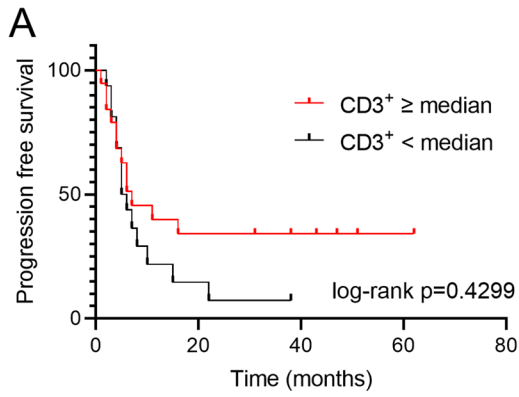


Fig. 4 Association between TIL phenotypes after CRT and PFS. The PFS of patients with esophageal squamous cell carcinoma was evaluated according to TIL phenotypes after CRT using the Kaplan–Meier analysis. The PFS curves of patients are shown, according to the densities of CD3⁺ (a), CD3⁺PD-1⁺ (b), CD3⁺CD8⁺ (c), CD3⁺CD8⁺PD-1⁺ (d), CD3⁺CD8⁺Foxp3⁻ (e), CD3⁺CD8⁺Foxp3⁻PD-1⁺ (f), and CD3⁺CD8⁺Foxp3⁺ lymphocytes (g) and CD206⁺ macrophages (h) in the tumor bed after CRT

CRT and underwent surgical resection [28–30]. A previous study showed that the number of tumor-infiltrating T cells in patients with ESCC who received neoadjuvant CRT was lower than that in patients who did not receive neoadjuvant CRT [28]. Paired transcriptome and mIHC analyses before and after neoadjuvant CRT were also reported [29]. This

study showed that immune scores and immune signaling pathways were enriched by transcriptome analysis after CRT, and mIHC analysis showed an increasing trend in the proportion of CD4⁺ Tconv cells in the TME after CRT in patients with ESCC [29]. In another study, single-cell RNA sequencing was performed to evaluate the cellular and molecular dynamics of neoadjuvant CRT in paired ESCC samples before and after CRT [30]. CRT increased CD8⁺ T-cell infiltration and promoted exhaustion in both major and minor responders. In major responders, CRT promoted the differentiation of Th cells but not Treg cells.

Clinical stages of ESCC are categorized as cT1–4aN0–3 according to the TNM classification or clinical stages I–III, which can be applied for CRT treatment. For stage I disease,

Table 3 Significance of clinicopathologic parameters and immune markers for PFS in patients with unresectable locally advanced ESCC

Variables		Univariate analysis			
		HR	95% CI	P value	
Age	≥ 65	1.20	0.23–6.30	0.823	
Sex	Male	0.45	0.08–2.47	0.361	
Tumor length, cm	≥ 6.5	1.57	0.34–71.75	0.558	
Lymphocyte count (before CRT) *	≥ 1470	0.42	0.07–2.38	0.324	
Lymphocyte count (after CRT) *	≥ 380	0.35	0.04–2.56	0.301	
TIL phenotypes before CRT					
CD3 ⁺ , /mm ²	≥ 150	0.99	0.46–2.09	0.969	
CD3 ⁺ PD-1 ⁺ , /mm ²	≥ 20	0.71	0.33–1.52	0.383	
CD3 ⁺ CD8 ⁻ , /mm ²	≥ 69	1.23	0.58–2.60	0.576	
CD3 ⁺ CD8 ⁻ PD-1 ⁺ , /mm ²	≥ 9	0.89	0.42–1.88	0.768	
CD3 ⁺ CD8 ⁺ , /mm ²	≥ 70	0.91	0.43–1.92	0.802	
CD3 ⁺ CD8 ⁺ PD-1 ⁺ , /mm ²	≥ 4	0.61	0.28–1.31	0.204	
CD3 ⁺ CD8 ⁻ Foxp3 ⁺ , /mm ²	≥ 3	2.56	1.16–5.65	0.019	
CD206 ⁺ , /mm ²	≥ 30	0.99	0.99–1.00	0.680	
TIL phenotypes after CRT					
CD3 ⁺ , /mm ²	≥ 312	0.60	0.28–1.29	0.191	
CD3 ⁺ PD-1 ⁺ , /mm ²	≥ 63	0.48	0.22–1.03	0.062	
CD3 ⁺ CD8 ⁻ , /mm ²	≥ 148	0.68	0.31–1.43	0.306	
CD3 ⁺ CD8 ⁻ PD-1 ⁺ , /mm ²	≥ 39	0.62	0.28–1.33	0.220	
CD3 ⁺ CD8 ⁺ , /mm ²	≥ 145	0.61	0.28–1.28	0.191	
CD3 ⁺ CD8 ⁺ PD-1 ⁺ , /mm ²	≥ 20	0.31	0.14–0.68	0.003	
CD3 ⁺ CD8 ⁻ Foxp3 ⁺ , /mm ²	≥ 5	2.37	1.05–5.34	0.036	
CD206 ⁺ , /mm ²	≥ 14	2.44	1.07–5.53	0.032	
Variables		Multivariate analysis			
		HR	95% CI	P value	
TIL phenotypes before CRT					
CD3 ⁺ CD8 ⁻ Foxp3 ⁺ , /mm ²	≥ 3	1.44	0.56	3.56	0.423
TIL phenotypes after CRT					
CD3 ⁺ CD8 ⁺ PD-1 ⁺ , /mm ²	≥ 20	0.33	0.14	0.77	0.010
CD3 ⁺ CD8 ⁻ Foxp3 ⁺ , /mm ²	≥ 5	1.57	0.62	3.98	0.336
CD206 ⁺ , /mm ²	≥ 14	1.87	0.79	4.44	0.151

P value < 0.05 was considered statistically significant

CRT has been investigated in patients with T1b stage for whom endoscopic treatment is difficult [31]. It has shown a high CR rate and preferable long-term prognosis, which are comparable to those of surgery; therefore, it is considered the standard treatment [32]. However, even a subset of cases in which cCR is achieved after CRT relapse [33, 34]. This is why the importance of surveillance and the need for additional treatment after definitive CRT has been reported [33]. The effectiveness of salvage surgery following definitive CRT has been demonstrated [35]. Preoperative CRT is often used as the standard treatment strategy for patients with locally advanced ESCC [36, 37]. Although surgical resection is an important therapeutic strategy for patients with cStage I–III, CRT is the only standard treatment for T4b and LNT4, despite of the fact that recurrence occurs at a rate of 45–53% even in CR cases [7, 33]. Accordingly, T4b and LNT4 were focused in this study to evaluate the sole efficacy of CRT [5, 38]. To the best of our knowledge, there have been no reports on the evaluation of paired samples from patients with unresectable locally advanced ESCC before and after CRT. In this study, we performed mIHC analysis on paired samples from patients with unresectable locally advanced ESCC before and after CRT. Supporting the results from previous studies on neoadjuvant CRT for patients with locally advanced esophageal cancer [13, 14, 28–30], we clarified that CRT increased tumor-infiltrating CD8⁺ T cells and CD4⁺ Tconv cells but decreased Treg cells and suppressive macrophages in patients with unresectable locally advanced ESCC. Simultaneously, CRT induced PD-1 expression in CD8⁺ T cells and CD4⁺ Tconv cells without the upregulation of terminally exhausted T-cell markers, such as TIGIT, LAG3, and Tim-3. In addition, the number of CD3⁺CD8⁺PD-1⁺ cells was significantly higher in patients with cCR than in those without cCR, which may be an independent predictor of cCR. PD-1 expression on CD8⁺ T cells is upregulated upon the recognition of high-affinity antigens [39], and PD-1⁺CD8⁺ T cells in tumors are predictive factors for the therapeutic response to PD-1 blockade therapy in lung and gastric cancers [39, 40]. These studies suggest that this may reflect the enhancement of antigen presentation by tumor-specific antigens in the TME by CRT.

The increase in CD3⁺CD8⁺PD-1⁺ cells after CRT observed in this study is an important finding that provides evidence for the need for PD-1 inhibitors after CRT. Several clinical trials have demonstrated the efficacy of combined CRT and PD-1 inhibitors [12, 41]. In addition, the TENERGY trial was introduced for unresectable locally advanced ESCC, and the results are awaited [42]. Moreover, tumor-associated macrophages (TAMs) and PD-1⁺ Tregs, which are defined as CD206⁺ and CD3⁺CD8⁺FoxP3⁺PD-1⁺ by immunohistochemistry, are associated with an unfavorable prognosis and can be decreased after CRT. A previous study showed low doses of RT (≤ 2 Gy) reprogram

TAMs to an M1 phenotype, which led to normalization of the tumor vasculature with a reduction of CD31⁺ vessels and upregulation of vascular cell adhesion protein-1 in tumor endothelium [43]. Other reports have shown that ICI responses are related to the number of TAMs or Tregs [44, 45]. In this study, CD3⁺CD8⁺PD-1⁺ cells were also increased in non-cCR after CRT (Online Resource 5). All of these findings suggest a rationale for additional ICI treatment after CRT, which may further improve prognosis.

This study had some limitations. For instance, the sample size was small because of the relatively low incidence of unresectable ESCC and the difficulty in obtaining a pair of tumor specimens before and after CRT. Another was the possibility of bias owing to intra-tumoral heterogeneity caused by endoscopic specimens. Taking this into account, we conclude that unresectable locally advanced ESCC can be immunologically activated by CRT. The abundance of CD8⁺PD-1⁺ cells after CRT is a favorable prognostic factor, suggesting a rationale for subsequent PD-1 inhibitor treatment. This study focused on patients with T4b and LNT4 to investigate the sole effect of CRT on ESCC, which can be applied to all stages of ESCC. These results can guide clinical trials to test the combination of immunotherapy and CRT.

Acknowledgements We thank all patients who participated in this study and their families and caregivers. We thank T. Takaku, K. Onagawa, M. Takemura, M. Hoshino, Y. Osada, C. Ozawa, and X. Takakura for their technical assistance.

Author contributions T. Habu, S. Kumagai, H. Bando, S. Koyama, and T. Kojima designed the study. T. Habu, S. Kumagai, and S. Koyama wrote the initial draft of the manuscript. T. Habu, S. Kumagai, H. Bando, S. Koyama, and T. Kojima contributed to the analysis and interpretation of the data and assisted in manuscript preparation. All the other authors contributed to the data collection, interpretation, and critical review of the manuscript. All authors have approved the final version of the manuscript and agreed to be accountable for all aspects of the study. We ensured that all questions related to the accuracy or integrity of any part of the study were appropriately investigated and resolved.

Funding This study was supported by a Grant-in-Aid for Scientific Research (C Grant No. 21K07252 [S. Koyama], JSPS Fellows no. 22KJ3156 [S. Kumagai], Early-Career Scientists no. 23K15088 [S. Kumagai], PAGES nos. 202130, 212126, 221184, and 231279 [S. Kumagai]); Japan Agency for Medical Research and Development (AMED)—the Moonshot Research and Development Program grant (no. 22zf0127009h0001 [H. Nishikawa, S. Koyama]); AMED—the Project for Promotion of Cancer Research and Therapeutic Evolution (P-PROMOTE no. 22ama221301h0001 [H. Nishikawa, S. Koyama.], no. 22ama221507h0001 [S. Kumagai], no. 23ama221329h0001 [S. Koyama]); AMED—the Practical Research for Innovative Cancer Control (no. 22ck0106724h0001 [H. Nishikawa, S. Koyama], no. 22ck0106773h0001 [S. Kumagai], no. 23ck0106796h0001 [S. Koyama]); Canon Foundation (S. Koyama.); Mitsubishi Foundation (S. Koyama.); Takeda Science Foundation (S. Kumagai); Taiju Life Social

Welfare Foundation (S. Kumagai); Astellas Foundation for Research on Metabolic Disorders (S. Kumagai); Senri Life Science Foundation (S. Kumagai); Uehara Memorial Foundation (S. Kumagai); Chugai Foundation for Innovative Drug Discovery Science (S. Kumagai); Japan Neurosurgical Society (S. Kumagai); and Japan Lung Cancer Society (a nonprofit organization) (S. Kumagai).

Declarations

Conflict of interest H. Bando reports honoraria from Ono Pharmaceutical, Taiho Pharmaceutical and Eli Lilly Japan. D. Kotani reports honoraria from Takeda, Chugai, Lilly, MSD, Ono, Seagen, Guardant Health, Eisai, Taiho, Bristol Myers Squibb, Daiichi-Sankyo, Pfizer, Merckbiopharma, and Sysmex, research funding from Ono, MSD, Novartis, Servier, Janssen, IQVIA, Syneoshealth, CIMIC, and Cimic-shifzero. M. Nakamura reports receiving personal fees from AstraZeneca and a research grant from illumina, outside the submitted work. S. Mitsunaga reports honoraria and research funding from Toray Industries, Pharmaceutical Co. Ltd., Chugai Pharmaceutical Co., Ltd., Astellas Pharma, Ajinomoto, Taiho Pharmaceutical Co., Ltd., PFDE-NA outside the submitted work, and personal fees from Ono Pharmaceutical Co. Ltd. outside the submitted work. H. Nishikawa received research funding and honoraria from Ono Pharmaceutical, Bristol-Myers Squibb, Chugai Pharmaceutical, and MSD, honoraria from Amgen and research funding from Taiho Pharmaceutical, Daiichi-Sankyo, Kyowa Kirin, Zenyaku Kogyo, Oncolys BioPharma, Debiopharma, Asahi-Kasei, Sysmex, Fujifilm, SRL, Astellas Pharmaceutical, Sumitomo Dainippon Pharma, and BD Japan outside of this study. S. Koyama has received research funding from Otsuka Pharmaceutical and Chugai Pharmaceuticals. T. Kojima reports receiving research funding from Beigene Ltd., AstraZeneca, Chugai Pharmaceutical, Parexel International, Shionogi, Taiho Pharmaceutical, Astellas Amgen BioPharma, MSD, and Ono Pharmaceutical; honoraria from Ono Pharmaceutical, Covidien Japan, MSD, Boehringer Ingelheim, Kyowa Kirin, EA Pharma, Bristol-Myers Squibb, 3H Clinical Trial, AstraZeneca, Taiho Pharmaceutical, Liang Yi Hui Healthcare Oncology News China, Japanese Society of Pharmaceutical Health Care and Sciences, Oncolys BioPharma, and BMS; advisory roles for Ono Pharmaceutical, Taiho Pharmaceutical, Japanese Society of Pharmaceutical Health Care and Sciences, and Liang Yi Hui Healthcare Oncology News China. All other authors have no conflicts of interest to disclose.

Ethical approval The study protocol was approved by the Institutional Review Board of the National Cancer Center (2021–2022). This study was conducted in accordance with the Declaration of Helsinki and the Japanese Ethical Guidelines for Medical and Health Research Involving Human Subjects.

References

- Sung H, Ferlay J, Siegel RL, et al. Global Cancer Statistics 2020: GLOBOCAN estimates of incidence and mortality worldwide for 36 cancers in 185 countries. *CA Cancer J Clin.* 2021;71:209–49.
- Shah MA, Altorki N, Patel P, et al. Improving outcomes in patients with oesophageal cancer. *Nat Rev Clin Oncol.* 2023;20:390–407.
- Grille VJ, Campbell S, Gibbs JF, Bauer TL. Esophageal cancer: the rise of adenocarcinoma over squamous cell carcinoma in the Asian belt. *J Gastrointest Oncol.* 2021;12:S339–49.
- Tahara M, Ohtsu A, Hironaka S, et al. Clinical impact of criteria for complete response (CR) of primary site to treatment of esophageal cancer. *Jpn J Clin Oncol.* 2005;35:316–23.
- Ohtsu A, Boku N, Muro K, et al. Definitive chemoradiotherapy for T4 and/or M1 lymph node squamous cell carcinoma of the esophagus. *J Clin Oncol.* 1999;17:2915–21.
- Shinoda M, Ando N, Kato K, et al. Randomized study of low-dose versus standard-dose chemoradiotherapy for unresectable esophageal squamous cell carcinoma (JCOG0303). *Cancer Sci.* 2015;106:407–12.
- Habu T, Kumanishi R, Ogata T, et al. Complete response to definitive chemoradiotherapy in unresectable locally advanced esophageal squamous cell carcinoma. *Esophagus.* 2023;20:533–40.
- Sun JM, Shen L, Shah MA, et al. Pembrolizumab plus chemotherapy versus chemotherapy alone for first-line treatment of advanced oesophageal cancer (KEYNOTE-590): a randomised, placebo-controlled, phase 3 study. *Lancet.* 2021;398:759–71.
- Doki Y, Ajani JA, Kato K, et al. Nivolumab combination therapy in advanced esophageal squamous-cell carcinoma. *N Engl J Med.* 2022;386:449–62.
- Kelly RJ, Ajani JA, Kuzdzal J, et al. Adjuvant nivolumab in resected esophageal or gastroesophageal junction cancer. *N Engl J Med.* 2021;384:1191–203.
- Bando H, Tsukada Y, Ito M, Yoshino T. Novel immunological approaches in the treatment of locally advanced rectal cancer. *Clin Colorectal Cancer.* 2022;21:3–9.
- Antonia SJ, Villegas A, Daniel D, et al. Durvalumab after chemoradiotherapy in stage III non-small-cell lung cancer. *N Engl J Med.* 2017;377:1919–29.
- Soeratrarn TT, Creemers A, Meijer SL, et al. Tumor-immune landscape patterns before and after chemoradiation in resectable esophageal adenocarcinomas. *J Pathol.* 2022;256:282–96.
- Kotsafti A, Scarpa M, Cavallin F, et al. Immune surveillance activation after neoadjuvant therapy for esophageal adenocarcinoma and complete response. *Oncoimmunology.* 2020;9:1804169.
- Brierley JD, Gospodarowicz MK, Wittekind C. *TNM classification of malignant tumours.* 8th ed. Wiley Blackwell; 2017.
- Japan ES. Japanese classification of esophageal cancer, 11th edition: part I. *Esophagus.* 2017;14:1–36.
- Eisenhauer EA, Therasse P, Bogaerts J, et al. New response evaluation criteria in solid tumours: revised RECIST guideline (version 1.1). *Eur J Cancer.* 2009;45:228–47.
- Kanda Y. Investigation of the freely available easy-to-use software “EZR” for medical statistics. *Bone Marrow Transplant.* 2013;48:452–8.
- Herter-Sprie GS, Koyama S, Korideck H, et al. Synergy of radiotherapy and PD-1 blockade in Kras-mutant lung cancer. *JCI Insight.* 2016;1: e87415.
- An L, Li M, Jia Q. Mechanisms of radiotherapy resistance and radiosensitization strategies for esophageal squamous cell carcinoma. *Mol Cancer.* 2023;22:140.
- Deng L, Liang H, Xu M, et al. STING-dependent cytosolic DNA sensing promotes radiation-induced type I interferon-dependent antitumor immunity in immunogenic tumors. *Immunity.* 2014;41:843–52.
- Fucikova J, Kepp O, Kasikova L, et al. Detection of immunogenic cell death and its relevance for cancer therapy. *Cell Death Dis.* 2020;11:1013.
- Apetoh L, Ghiringhelli F, Tesniere A, et al. Toll-like receptor 4-dependent contribution of the immune system to anticancer chemotherapy and radiotherapy. *Nat Med.* 2007;13:1050–9.
- Sato H, Niimi A, Yasuhara T, et al. DNA double-strand break repair pathway regulates PD-L1 expression in cancer cells. *Nat Commun.* 2017;8:1751.
- Haddad R, Zlotnik O, Goshen-Lago T, et al. Tumor lymphocyte infiltration is correlated with a favorable tumor regression grade after neoadjuvant treatment for esophageal adenocarcinoma. *J Pers Med.* 2022;12:627.

26. Zingg U, Montani M, Frey DM, et al. Tumour-infiltrating lymphocytes and survival in patients with adenocarcinoma of the oesophagus. *Eur J Surg Oncol*. 2010;36:670–7.
27. Koemans WJ, van Dieren JM, van den Berg JG, et al. High CD8(+) tumour-infiltrating lymphocyte density associates with unfavourable prognosis in oesophageal adenocarcinoma following poor response to neoadjuvant chemoradiotherapy. *Histopathology*. 2021;79:238–51.
28. Zingg U, Montani M, Frey DM, et al. Influence of neoadjuvant radio-chemotherapy on tumor-infiltrating lymphocytes in squamous esophageal cancer. *Eur J Surg Oncol*. 2009;35:1268–72.
29. Park S, Joung JG, Min YW, et al. Paired whole exome and transcriptome analyses for the Immunogenomic changes during concurrent chemoradiotherapy in esophageal squamous cell carcinoma. *J Immunother Cancer*. 2019;7:128.
30. Wen J, Fang S, Hu Y, et al. Impacts of neoadjuvant chemoradiotherapy on the immune landscape of esophageal squamous cell carcinoma. *EBioMedicine*. 2022;86: 104371.
31. Minashi K, Nihei K, Mizusawa J, et al. Efficacy of endoscopic resection and selective chemoradiotherapy for stage I esophageal squamous cell carcinoma. *Gastroenterology*. 2019;157:382–90 (e3).
32. Kato K, Ito Y, Nozaki I, et al. Parallel-group controlled trial of surgery versus chemoradiotherapy in patients with stage I esophageal squamous cell carcinoma. *Gastroenterology*. 2021;161:1878–86 (e2).
33. Sudo K, Xiao L, Wadhwa R, et al. Importance of surveillance and success of salvage strategies after definitive chemoradiation in patients with esophageal cancer. *J Clin Oncol*. 2014;32:3400–5.
34. Motoori M, Yano M, Ishihara R, et al. Comparison between radical esophagectomy and definitive chemoradiotherapy in patients with clinical T1bN0M0 esophageal cancer. *Ann Surg Oncol*. 2012;19:2135–41.
35. Takeuchi H, Ito Y, Machida R, et al. A single-arm confirmatory study of definitive chemoradiation therapy including salvage treatment for clinical stage II/III esophageal squamous cell carcinoma (JCOG0909 study). *Int J Radiat Oncol Biol Phys*. 2022;114:454–62.
36. Yang H, Liu H, Chen Y, et al. Long-term efficacy of neoadjuvant chemoradiotherapy plus surgery for the treatment of locally advanced esophageal squamous cell carcinoma: the NEOCRTEC5010 randomized clinical trial. *JAMA Surg*. 2021;156:721–9.
37. van Hagen P, Hulshof MC, van Lanschot JJ, et al. Preoperative chemoradiotherapy for esophageal or junctional cancer. *N Engl J Med*. 2012;366:2074–84.
38. Cooper JS, Guo MD, Herskovic A, et al. Chemoradiotherapy of locally advanced esophageal cancer: long-term follow-up of a prospective randomized trial (RTOG 85–01). *Radiat Ther Oncol Group JAMA*. 1999;281:1623–7.
39. Kumagai S, Togashi Y, Kamada T, et al. The PD-1 expression balance between effector and regulatory T cells predicts the clinical efficacy of PD-1 blockade therapies. *Nat Immunol*. 2020;21:1346–58.
40. Thommen DS, Koelzer VH, Herzig P, et al. A transcriptionally and functionally distinct PD-1(+) CD8(+) T cell pool with predictive potential in non-small-cell lung cancer treated with PD-1 blockade. *Nat Med*. 2018;24:994–1004.
41. Kim S, Boustani J, Vernerey D, et al. Phase II INTERACT-ION study: ezabenlimab (BI 754091) and mDCF (docetaxel, cisplatin, and 5-fluorouracil) followed by chemoradiotherapy in patients with Stage III squamous cell anal carcinoma. *Front Oncol*. 2022;12: 918499.
42. Bando H, Kotani D, Tsushima T, et al. TENERGY: multicenter phase II study of Atezolizumab monotherapy following definitive Chemoradiotherapy with 5-FU plus Cisplatin in patients with unresectable locally advanced esophageal squamous cell carcinoma. *BMC Cancer*. 2020;20:336.
43. Klug F, Prakash H, Huber PE, et al. Low-dose irradiation programs macrophage differentiation to an iNOS⁺/M1 phenotype that orchestrates effective T cell immunotherapy. *Cancer Cell*. 2013;24:589–602.
44. Peranzoni E, Lemoine J, Vimeux L, et al. Macrophages impede CD8 T cells from reaching tumor cells and limit the efficacy of anti-PD-1 treatment. *Proc Natl Acad Sci USA*. 2018;115:E4041–50.
45. Arlauckas SP, Garris CS, Kohler RH, et al. In vivo imaging reveals a tumor-associated macrophage-mediated resistance pathway in anti-PD-1 therapy. *Sci Transl Med*. 2017. <https://doi.org/10.1126/scitranslmed.aal3604>.

Publisher's Note Springer Nature remains neutral with regard to jurisdictional claims in published maps and institutional affiliations.

Springer Nature or its licensor (e.g. a society or other partner) holds exclusive rights to this article under a publishing agreement with the author(s) or other rightsholder(s); author self-archiving of the accepted manuscript version of this article is solely governed by the terms of such publishing agreement and applicable law.